

INTERNATIONAL SOCIETY FOR SOIL MECHANICS AND GEOTECHNICAL ENGINEERING



This paper was downloaded from the Online Library of the International Society for Soil Mechanics and Geotechnical Engineering (ISSMGE). The library is available here:

<https://www.issmge.org/publications/online-library>

This is an open-access database that archives thousands of papers published under the Auspices of the ISSMGE and maintained by the Innovation and Development Committee of ISSMGE.

Water, heat and electric current flow in saturated and unsaturated sandy soil

T. Tokoro

Department of Engineering for Innovation, National Institute of Technology, Tomakomai College, Japan

T. Ishikawa

Faculty of Engineering, Hokkaido University, Sapporo, Japan

ABSTRACT: Heat flow, electric current flow and substance flow such as water and solution flow in soils can depend on the water contents. Each geotechnical parameter like thermal conductivity, permeability coefficient and electric resistivity have been investigated from the viewpoint of the dependency of water content. However, although apparently these parameters have strong relation with each other, the relationships among the parameters are not clarified since each testing methods for unsaturated soils are complicated and not easy to carry out, and they require a long time to perform. In this study, three types of tests which determine the parameters mentioned i.e., water permeability, thermal conductivity and electrical resistivity were performed for Toyoura sand under saturated and unsaturated conditions. Water retention test was also conducted to compare the values with the soil-water characteristic curve (SWCC). According to the test results, the thermal conductivity, the electrical resistivity and the permeability of a sandy soil have similar tendency that they have an inflection point at the water saturation corresponding to the changing point between pendular saturation and fuzzy saturation. The slight difference in the inflection point might be caused by the water distribution in soil.

1 INTRODUCTION

The characteristics of soils strongly depend on water content. Aside from the difference between saturated and unsaturated conditions, mechanical properties are different under different water contents. Therefore, the study about the mechanical properties of unsaturated soils has been vigorously advanced. Moreover, transfer of materials such as water, thermal propagation and electric current flow in soils depend on water contents since pore water works as a medium. These flowability in soils also depends on the water content. Certain thickness of water film around soil particle is necessary for the flow of heat, water and electric current. In addition to the effect of water content on the mechanical properties of soils, it is necessary to grasp the effect of water content on flowability. For this reason, water, heat and electric current flows through unsaturated and saturated soils have been researched as with mechanical properties. The characteristics of the parameters above mentioned have been clarified respectively, and some predicting models have been developed. For example, the Mualem's equation (Mualem 1976) has been widely used to estimate the permeability of unsaturated soils by using soil-water characteristics curve (SWCC). Lu and Dong (2015) focused attention on the strong relationship between thermal conduc-

tivity and the soil-water characteristic curve and proposed a closed-form equation by applying the van Genuchten model (van Genuchten, 1980). When it comes to usage of electric resistance, Archie (1942, 1947) developed an equation for rock that can estimate the permeability coefficient by using the resistance. Furthermore, Tokoro et al. (2016) clarified the relationship between thermal conductivity and electrical resistance and developed an estimation equation. However, there are very few researches attempted to show all the parameters of the same soil with same dry density. The authors conducted the water permeability test, thermal conductivity test and electrical resistance test for Toyoura sand of the same dry density in previous studies (Ishikawa et al. 2010; Tokoro et al. 2016).

In this study, the parameters such as permeability coefficient, SWCC, thermal conductivity and electrical resistance are compared to grasp the relation among them to explore the possibility that each parameter can be estimated by other parameters.

2 MATERIAL AND METHODS

2.1 Material

The material used in this study is Toyoura sand, which has been widely used in Japan. The grain size distribution and the physical properties of Toyoura sand are shown in Figure 1 and Table 1.

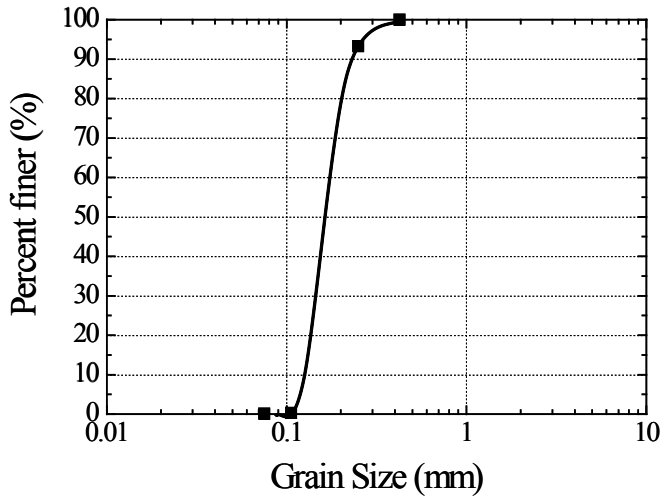


Figure 1. Grain size distribution.

Table 1. Physical properties of Toyoura sand.

Physical properties	
Soil particle density(g/cm ³)	2.65
Maximum dry density(g/cm ³)	1.65
Minimum dry density(g/cm ³)	1.35
Average grain diameter(mm)	0.18
Fine content (%)	0

2.2 Thermal conductivity test device

In this study, the single probe method which is an unsteady state method was adopted. Figure 2a shows a schematic diagram of the thermal conductivity device. The device consists of a heat probe, a data logger and a DC power supply. Detailed drawing of the heat probe is shown in Figure 2b, which consists of a copper pipe (150 mm height and 3 mm diameter), a constantan wire as heater and T type thermocouple. The remaining space was filled with paraffin.

The probe induces heat by applying voltage to the constantan wire, and temperature rise of the probe can be measured with the inserted thermocouple. The principle of the single probe method is that the temperature rise in the probe depends on the thermal conductivity of the specimen in which the probe is inserted. Thermal conductivity is calculated by using Equation (1).

$$\lambda = \frac{Q}{4\pi\Delta\theta} \ln\left(\frac{t_2}{t_1}\right) \quad (1)$$

where λ = thermal conductivity (W m⁻¹K⁻¹); Q = heat per unit length (W/m); t_1, t_2 = time (s); $\Delta\theta$ = Increase in temperature (°C).

2.3 Permeability test apparatus

A triaxial apparatus for permeability testing of unsaturated soil using the pressure membrane method has been developed to shorten the testing time. Figure 3a shows a schematic diagram of the apparatus. The apparatus mainly consists of a triaxial

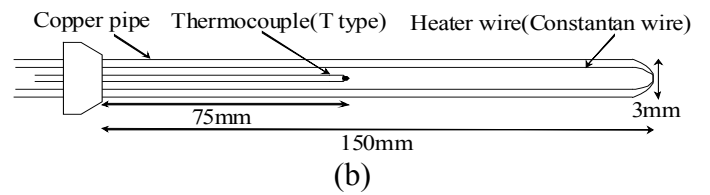
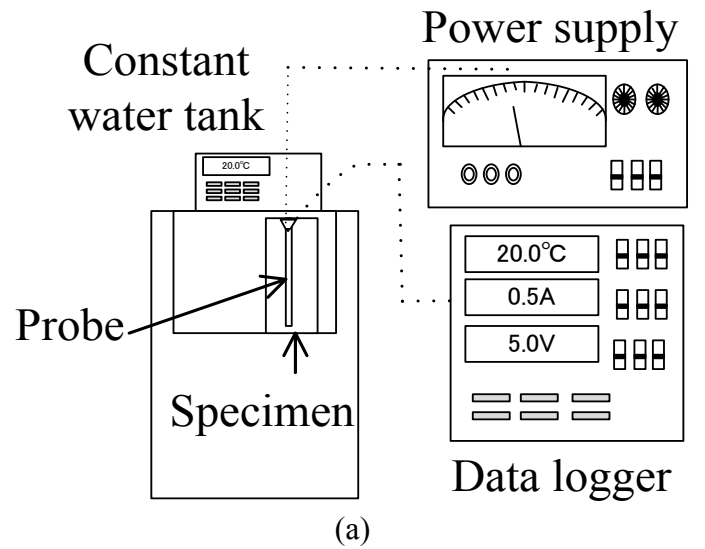


Figure 2. Thermal conductivity test device: a) Schematic of thermal conductivity test device, b) Detailed drawing of thermal probe

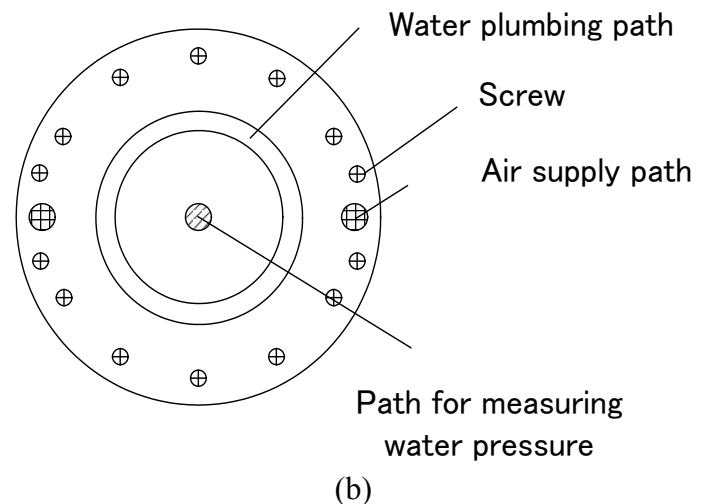
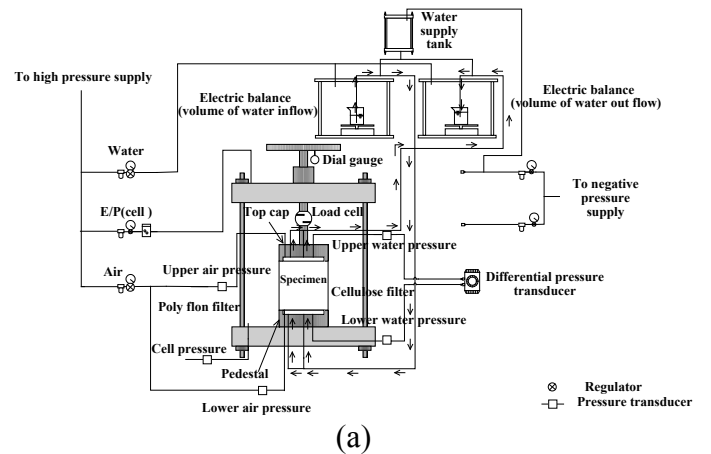


Figure 3. Permeability test apparatus: a) schematic diagram of the permeability apparatus, b) structure of cap and pedestal.

cell, electric balances (sensitivity is 1 mg), which were set in a compression chamber, pressure transducer, differential pressure transducer, electric/pressure transducer, regulator, thermometer and so on. As the apparatus is a modified apparatus of the Richards type (Richard & Moore, 1952), it can perform the permeability test using the steady state method and the water retention test simultaneously. Figure 3b shows the top cap and bottom pedestal. The apparatus can control the pore water pressure and pore air pressure respectively. Moreover, the apparatus can measure the pore water pressure because the path to measure water pressure is independent of the path used to control it.

In this apparatus, a versapor membranes filter of AEV = 60 kPa and 200 kPa are used to control and measure the pore water pressure. Hydrophobic polyflon filter which is made from polytetrafluoroethylene (PTFE) is used for controlling the pore air pressure. These filters were secured by a fixing plate.

2.4 Electrical conductivity test

The four-electrode technique is used to measure the electrical resistance. Figure 4 illustrates the electrical conductivity test device. A cylindrical cell made with polyvinyl chloride with 150 mm in height and 56 mm in diameter is used. Two supplying electrodes (current electrodes) and two measuring electrodes (potential electrodes) are used separately. The length between two measuring electrodes L is 100 (mm). The electrical resistance is calculated using Equation (2):

$$r = \frac{VA}{IL} \quad (2)$$

where r = the electric resistance (Ωm); V = the voltage measured between two measuring electrodes (V); I = the current measured between the measuring electrodes (A); A = the cross section of the area (mm^2).

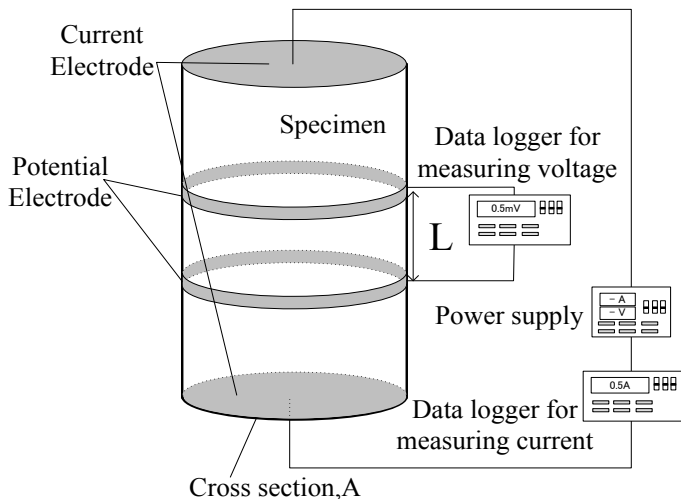


Figure 4. Electric conductivity test device.

3 METHODOLOGY

3.1 Thermal conductivity test

The soils with adjusted moisture contents are put in stainless steel cylindrical containers (180 mm in height and 72 mm in diameter) and compacted to achieve prescribed dry densities as Toyoura sand; $\rho_d=1.59 \text{ g/cm}^3$. To achieve a constant temperature, each specimen is kept in a constant-temperature water tank at 20 °C. After a constant temperature is obtained, a voltage is supplied to the constantan wire for 2 minutes and the temperature-increment of the probe is measured. The heat per unit length is set to 12 W/m to control the temperature-change to less than 6 °C during the test. The gradient of the relationship between temperature increase and elapsed time ($\Delta\theta/\ln(t_2/t_1)$) is obtained by the least-squares method. Thermal conductivity is calculated by substituting the gradient and heat per unit length into Equation (1).

3.2 Electrical conductivity test

Similar to the thermal conductivity test, soil with an adjusted moisture content placed in a cylindrical cell (height 150 mm in height and 56 mm in diameter) is compacted to obtain the same dry densities as the thermal conductivity test specimen. After sample-specimen preparation, a voltage is applied to electrodes (current electrodes) at both ends of the specimen and the current and voltage are measured by current and potential electrodes (Figure 4). The electrical resistance is calculated by Equation (2) using the measured voltage and current.

3.3 Permeability test

Test specimens were prepared by using the air pluviation method. The dry density after consolidation was aimed at 1.59 g/cm^3 . After setting the test specimen in a triaxial cell, de-aired water was permeated into the voids until the degree of saturation (S_r) became 85 %. After permeating water into the specimen, a confining pressure (σ_c) of 99 kPa, pore water pressure (u_w) of 50 kPa and pore air pressure (u_a) of 50kPa was applied to the specimen to consolidate the specimen under the net normal stress (σ_{net}) of 49 kPa. The net normal stress is defined as $\sigma_{net}=\sigma_c-u_a$. The test specimen is column-shaped, with 70 mm in diameter and 30mm in height.

The procedure for carrying out the unsaturated permeability test is described as follows. After consolidation, a differential head (Δh) of 1 cm between top and bottom of specimen was set, considering the frictional head loss in the water plumbing line, and the net normal stress (σ_{net}) of 49 kPa was kept constant.

The apparatus can keep the head given across the specimen constant during the permeability test using

a Mariotte bottle. Evaporation of moisture from the beaker was prevented by means of floating oil on water. Here, positive amount of absorption (ΔQ_1) and drainage (ΔQ_2) are defined as absorption and drainage respectively. Steady state was attained when the amount of absorption in the bottom of the specimen (ΔQ_1) became equal to amount of drainage (ΔQ_2) as shown in Equation 3. A series of tests were conducted at room temperature.

$$\Delta Q_1 = \Delta Q_2 = q \quad (3)$$

The permeability coefficient (k_w) was calculated from the following Equation 4 using the water flow rate (q), which was measured by electric balances and the differential head (Δh), which was measured by a differential pressure transducer. In this study, the pore air pressure of the specimen was not measured directly; instead, values obtained by pressure transducers at the upper and lower air paths were used for experimental data.

$$k_w = \frac{qL}{A \cdot \Delta h \cdot 60 \cdot 100} \quad (4)$$

where k_w = permeability coefficient; q = water flow rate; L = length of specimen; A = cross section; Δh = differential head.

Keeping net normal stress of 49 kPa, confining pressure and pore air pressure were increased to alter suction. The above procedure was repeated for different moisture content in specimens. The permeability coefficient for the soil-water characteristic curve on the drying path was obtained. Moreover, the soil-water characteristic curve was obtained by means of calculating the moisture content from the amount of absorption and drainage measured by the electric balances.

4 RESULT AND DISCUSSION

4.1 Thermal conductivity

Figure 5 shows the thermal conductivity of Toyoura sand. The thermal conductivity of the soil increases with moisture-content growth. The relationship between thermal conductivity and moisture content is however nonlinear and the change rate of thermal conductivity along with moisture content is not constant as previous studies have shown. Thermal flow was conducted through soil particles and pore water because the thermal conductivity of air is low. Thermal conductivity is therefore likely proportional to the moisture content, since the thermal conductivity of soil depends on its moisture content even with identical dry densities. For example, Kamoshida et al. (2013) indicated results that were similar to those of this study for the relationship between thermal conductivity and moisture content and they presumed that water at lower moisture content does not

contribute to thermal conduction. This is thought to be because most pore water does not continue at lower moisture content than the inflection point.

4.2 Electric resistance

Figure 6 shows the electric resistivity of Toyoura sand. Even corresponding inflection points of moisture content are slightly different, electric resistance and thermal conductivity have the same trend that the value drastically changes at certain moisture water content. Furthermore, the inflection points of both thermal conductivity and electrical resistance approximately agree with each other. Similar mechanisms are behind the nonlinear relationship between moisture content and either thermal conductivity or electrical resistance.

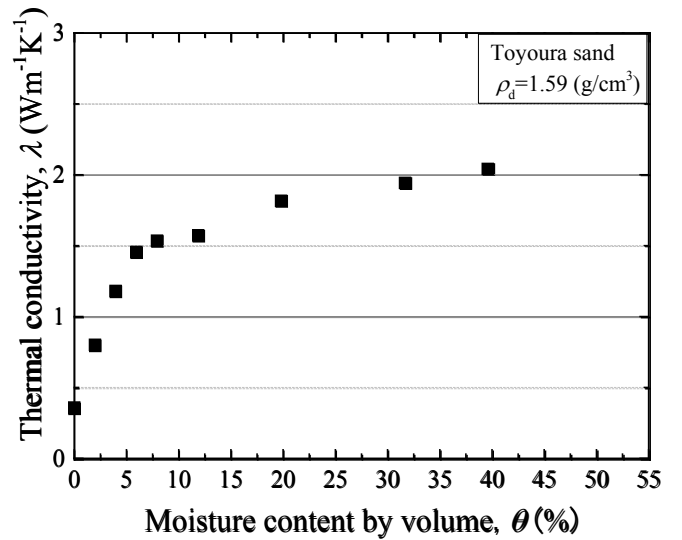


Figure 5. Thermal conductivity.

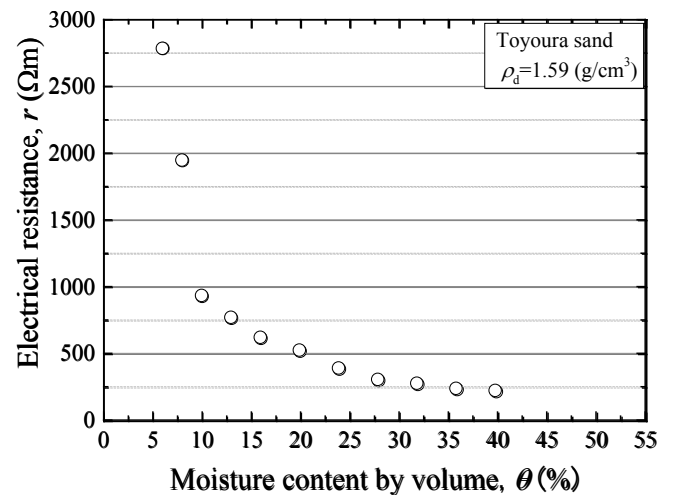


Figure 6. Electrical resistance.

4.3 Permeability coefficient and soil water characteristics curve

Figure 7 and Figure 8 show the permeability coefficient and SWCC respectively, obtained simultaneously by the constant head permeability test. The permeability decreases towards dry condition from quasi-saturated water content. Compared with SWCC, the permeability coefficient decreases linearly on the single logarithmic plot until the water contents became less than pendular water saturation. The permeability coefficient drastically changes at the water content corresponding to the changing point of SWCC.

4.4 Comparison of each value

The thermal conductivity, the electrical resistance and the permeability coefficient changed drastically at the water content corresponding to the changing point between pendular saturation and fuzzy saturation on the SWCC. Figure 9 shows the comparison of the inflection points. Even though there are slight differences in the drastic changing points among them, the point almost agrees with each other. Since the dry densities of the specimens for each test were almost the same, the slight differences might be attributable to the different way of conducting in soils.

As for the magnitude relation of the inflection points, those of thermal conductivity and electrical resistance are lower compared with the permeability. These differences might depend on water thickness. Figure 10 shows the estimated pore water condition in soils. Under less water than pendular water saturation, water exists as absorbed water (see Figure 10a). Even though water content is quite low, thin water film is thought to cover soil particle which is absorbed water. Under this water condition, heat, water and electric current hardly flow in the soil because of the shortage of water content.

When water increase from the water condition, water can be assigned between soil particles as meniscus water (see Figure 10b). As for thermal flow, thin water film and meniscus water works as heat medium. Therefore, thermal conductivity increases drastically at this water contents. On the other hand, it is assumed that the discontinuous meniscus water doesn't contribute to the electric current and water flow since water thickness is almost the same as the previous water condition. Therefore, the inflection point of the thermal conductivity is lowest in the parameters.

The next step of the water condition from the condition of Figure 10b shows in Figure 10c. Under this water condition, water mostly can be continuous and water thickness can get to be thick so that electric current and water flow are easier to conduct drastically. One of the reasons that the inflection point of the permeability is the highest in the parameters is

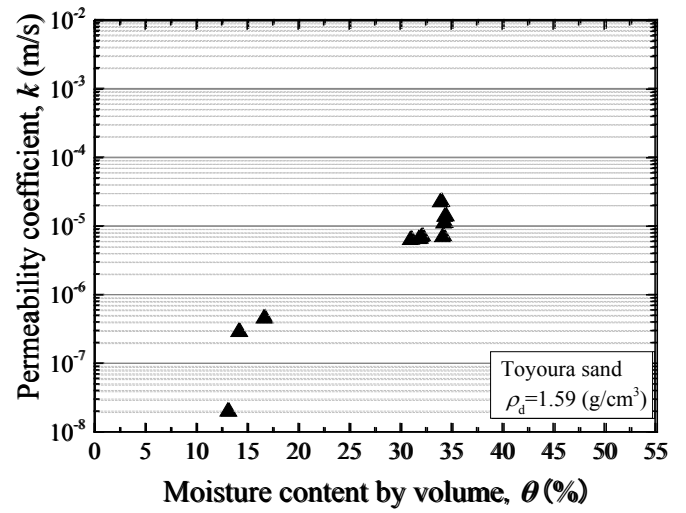


Figure 7. Permeability coefficient.

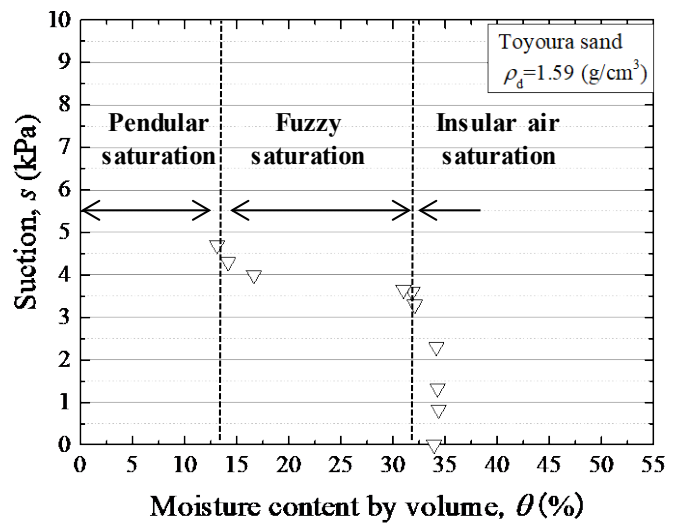


Figure 8. Soil water characteristic curve.

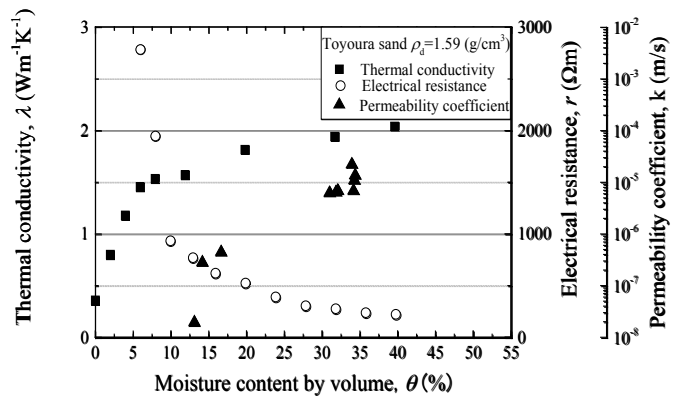


Figure 9. Comparison of inflection point.

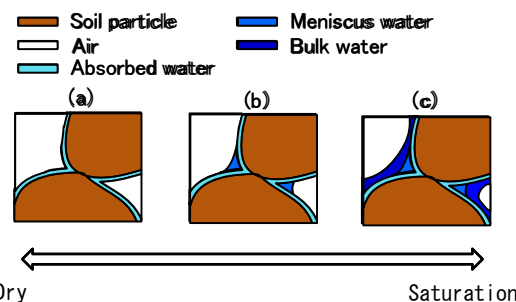


Figure 10. Pore water condition in unsaturated soil.

due to the suction since suction is not thought to affect thermal conductivity and electric flow.

As mentioned above, thermal conductivity, electrical resistance and permeability coefficient have strong relations based on the water distribution in soil. Archie (1942, 1947) developed a simple equation that can estimate the permeability with electrical resistance. However, Nishida and Aoyama (1993) revealed that the equation made by the predicting equation have no applicability to the permeability of coefficient on the drain process. This indicates that water form in soil and its function should be considered to make a predicting model. In other words, there is a possibility that permeability of coefficient can also be estimated by the electrical resistance, obtained by the easiest test among the tests, if the differences are taken into consideration.

5 CONCLUSIONS

In this study, thermal conductivity, electrical resistivity, the permeability coefficient and SWCC obtained by previous study the authors conducted before were compared.

The thermal conductivity, the electrical resistivity and the permeability of a sandy soil have similar tendency that they have an inflection point at the water saturation corresponding to the changing point between pendular saturation and fuzzy saturation.

The slight difference in the inflection point might be caused by the water distribution in soils. There is a possibility that each parameter can be predicted by other parameters if the difference would be considered.

6 REFERENCES

- Archie, G.E. 1942. The electrical resistivity log as an aid in determining some reservoir characteristics. *Transactions of the AIME* 146(1): 54-62.
- Archie, G.E. 1947. Electrical resistivity as an aid in core analysis interpretation. *Bulletin of the American Association of Petroleum Geologists*, AIME 31(2): 350-366.
- Ishikawa, T., Tokoro, T., Ito, K. & Miura, S. 2010. Testing methods for hydro-mechanical characteristics of unsaturated soils subjected to one-dimensional freeze-thaw action. *Soils and Foundations* 50(3): 431-440.
- Kamoshida, T., Hamamoto, S., Kawamoto, K., Sasaki, T. & Komatsu, T. 2013. Thermal properties of sands at variably-saturated condition: Effects of particle size and shape, and quartz content. *Journal of the Japanese Society of Soil Physics* (124): 11-16.
- Nishida, I. & Aoyama, C. 1993. The characteristics of resistivity of the unsaturated soil and the application of electric prospecting for evaluation of seepage flow through the ground. *Journal of JSCE* 475: 1-9.
- Lu, N. & Dong, Y. 2015. Closed-form for thermal conductivity of unsaturated soils at room temperature. *Journal of Geotechnical and Geoenvironmental Engineering*, ASCE 141(6): 04015016.
- Mualem, Y. 1972. A new model for predicting the hydraulic conductivity of unsaturated porous media. *Water Resources Research* 12(3): 513-522.
- Richards, L.A. & Moore, D.C. 1952. Influence of capillary conductivity and depth of wetting on moisture retention test. *Transactions of the American Geophysical Union* 33(4): 531-540.
- Tokoro, T., Ishikawa, T., Shirai, S. & Nakamura, T. 2016. Estimation methods of soil thermal conductivity with electric characteristics. *Soils and Foundations* 56(5): 943-952.
- van Genuchten, M.T. 1980. A closed-form equation for predicting the hydraulic conductivity of unsaturated soils. *Soil Science Society of America Journal* 44(5): 892-898.